in vivo *28*: 189-196 (2014)

Effects of Mouse Genotype on Bone Wound Healing and Irradiation-induced Delay of Healing

JULIE GLOWACKI[1], SHUICHI MIZUNO[1], JASON KUNG[1], JULIE GOFF[2], MICHAEL EPPERLY[2], TRACY DIXON[2], HONG WANG[2] and JOEL S. GREENBERGER[2]

[1]*Department of Orthopedic Surgery, Brigham and Women's Hospital, Harvard Medical School, Boston, MA, U.S.A.;*
[2]*Department of Radiation Oncology, University of Pittsburgh Cancer Institute, Pittsburgh, PA, U.S.A.*

Abstract. *We tested the effects of mouse genotype (C57BL/6NHsd, NOD/SCID, SAMR1, and SAMP6) and ionizing irradiation on bone wound healing. Unicortical wounds were made in the proximal tibiae, and the time course of spontaneous healing and effects of irradiation were monitored radiographically and histologically. There was reproducible healing beginning with intramedullary osteogenesis, subsequent bone resorption by osteoclasts, gradual bridging of the cortical wound, and re-population of medullary hematopoietic cells. The most rapid wound closure was noted in SAMR1 mice, followed by SAMP6, C57BL/6NHsd, and NOD/SCID. Ionizing irradiation (20 Gy) to the leg significantly delayed bone wound healing in mice of all four genotypes. Mice with genetically-determined predisposition to early osteopenia (SAMP6) or with immune deficiency (NOD/SCID) had impairments in bone wound healing. These mouse models should be valuable for determining the effects of irradiation on bone healing and also for the design and testing of novel bone growth-enhancing drugs and mitigators of ionizing irradiation.*

Bone tissue has a remarkable capacity for post-natal regeneration, but there are many circumstances that delay or prevent fracture healing, including therapeutic irradiation, aging, or bone injury combined with exposure to ionizing irradiation (1-3). Radiation is known to cause complications in skeletal tissue and to adversely-affect the quality of life in cancer survivors (4). In the setting of preoperative chemoradiotherapy to facilitate removal of bone tumors, delayed fracture healing may follow (5). Although there are known impairments in both the rate and quality of bone healing of irradiated bone, the genetic and environmental factors that influence the process are unknown. In addition, the development of agents to stimulate compromised bone healing may require modification in patients who have had irradiation to a surgical or pathogenic site.

In these mice studies, we sought to determine the influence of genotype on both the process of bone healing, and the effect of ionizing irradiation thereupon. We previously developed a rat model of tibial osseous wounds to test implants that would hinder spontaneous healing and that would overcome hindrances (6, 7). In this model, circular, unicortical osseous wounds heal centripetally, with a time-dependent decrease in cortical wound diameter following the resorption of temporary intramedullary ossification. We adapted the model for C57BL/6NHsd mice and demonstrated delayed bone healing by ionizing irradiation to the leg, in a dose-dependent fashion (8). Furthermore, amelioration of the irradiation-induced delay in bone wound healing was achieved with a single intraperitoneal dose of the hemigramicidin-based GS-nitroxide antioxidant, JP4-039.

We chose mouse models representative of accelerated osteopenia (SAMP6 mice) (9, 10) and of immunological deficiency (NOD/SCID mice) (11), for comparison with the more standard C57BL/6NHsd mouse. We evaluated the time course of unicortical bone wound healing in the proximal tibia compared to that in control mice of the same gender and age and measured the effects of ionizing irradiation to one leg on bone wound healing. The results demonstrate genotype-specific influences on both the kinetics of bone wound healing and the delay in healing due to ionizing irradiation of the wound site.

Materials and Methods

Mice. Mice were obtained from Harlan Laboratories (Indianapolis, IN, USA) and were bred, housed, and studied in accordance with Institutional Animal Care and Use Committee protocol number 1111220B, approved at the University of Pittsburgh Cancer Institute.

Correspondence to: Julie Glowacki, Ph.D., Orthopedic Research, Brigham and Women's Hospital, 75 Frances Street, Boston, MA 02115, U.S.A. Tel: +1 6177326885, e-mail: jglowacki@partners.org

Key Words: Bone wound healing, irradiation, C57BL/6NHsd, NOD/SCID, SAMP6 mice, genotype.

C57BL/6NHsd and NOD/SCID mice were studied between six and eight weeks of age; SAMP6 and SAMR1 mice were between four and five months of age. Different numbers of mice were available for experiments due to differences in breeding rates and schedules. Data for subsets of males and females were pooled because analysis revealed no statistical differences between them. Irradiation, wound creation, and radiographic measurements were performed at the University of Pittsburgh. Drug and irradiation delivery to subgroups occurred 24 h before unicortical osseous wounds were created. Mice treated with JP4-039 or with vehicle were exposed to radiation 10 min after drug delivery. The synthesis of JP4-039 was described previously (12, 13). JP4-039 was dissolved in a solution of 45% 2-hydroxypropyl-B-cyclodextrin and 55% water. Subgroups of mice were injected intraperitoneally with 100 μl of JP4-039 at a dose of 10 mg/kg. Control mice were injected intraperitoneally with the vehicle cyclodextrin.

Unicortical tibial wounds. The model of osseous wound healing was based on a model of spontaneous tibial wound repair in adult rats (6) and developed by us for C57BL/6NHsd mice (8). Mice were anesthetized intraperitoneally with phenobarbital (220-250 μl, 1:10 dilution in water, 70 mg/kg). Some groups of mice were irradiated before wound creation. A 15-mm skin incision was created laterally to the anterior tibial crest and exposure of the lateral tibia was achieved by retraction of overlying tissue. A handheld engraving drill (Dremel, Racine, WI, USA) with a 1.2-mm cutting bit (Dremel) was used to create a round, unicortical osseous wound at 5-mm below the proximal epiphysis. The wound was irrigated with cold phosphate-buffered saline (PBS, 1×; Mediatech, Herndon, VA, USA) to remove bone dust and fragments. After reapproximation of the soft tissue envelope, the skin was closed with 9 mm stainless steel wound clips (Becton Dickinson, Sparks, MD, USA).

Irradiation. Phenobarbital was used to anesthetize mice while the right hind limbs were immobilized with tape. Delivery of single fraction of 20 Gy doses was carried out by a 6-MV linear accelerator (Varian Corporation, Palo Alto, CA, USA), confined to a 38×2 cm irradiation field at a source-to-bolus distance of 100 cm. To ensure homogeneity of dose to the bone, one centimeter of tissue-equivalent bolus was placed on top of the leg and thermoluminescent dosimeters were used to confirm the accuracy of dose delivery.

Radiographic measurements of wound healing. Radiographs of the lateral tibial aspects were taken with a 35 kV x-ray machine (MX-20, Faxitron X-ray LLC., Lincolnshire, IL, USA) at x1.5 magnification. Radiographs (Kodak BioMax XAR, Rochester, NY, USA) were imported into Adobe Photoshop CS3 (Adobe Systems Inc., San Jose, CA, USA). Wound diameter was calculated by measuring and converting the number of pixels that spanned the wound into millimeters (one pixel=1/100 of a millimeter) using software within the package. Measurements were made in triplicate and averaged for statistical analysis.

Histology. The mouse tibias were fixed in 2% paraformaldehyde in 0.1M cacodylate buffer (pH 7.4) at 4˚C for one week, rinsed in 0.1 M cacodylate buffer, then de-calcified in a 7.5% ethylenediamine tetra-acetate (EDTA). The EDTA solution was refreshed every other day for the first week, then twice each week thereafter, until the bones were pliable. Specimens were embedded in 2-hydroxyethyl methacrylate (Technovit 7100; Heraeus Kulzer, Wehrheim, Germany). Six-micrometer transverse or longitudinal sections were stained with toluidine blue for cellular and tissue analyses and for localization of tartrate-resistant acid phosphatase (TRAP) enzymatic activity as an index of osteoclastic bone resorption (14). Histological processing and examinations were carried out at the Brigham and Women's Hospital.

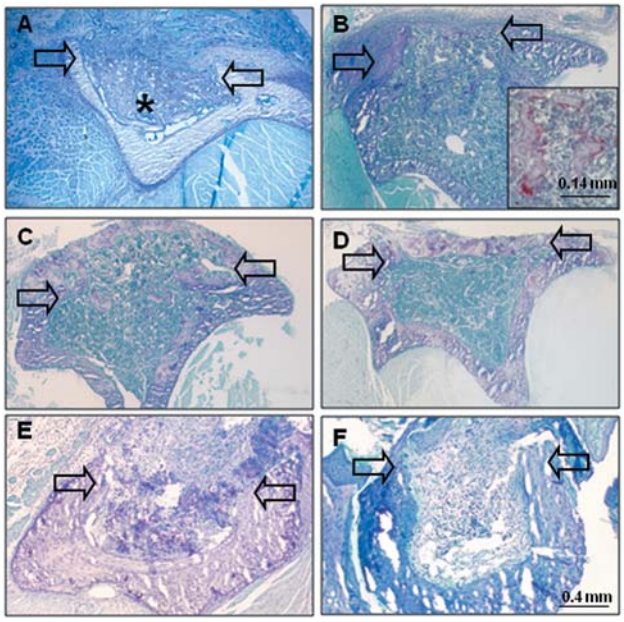

Figure 1. *Histological evaluation of spontaneous repair of tibial wounds in C57BL/6NHsd (A-D), compared with NOD/SCID (E-F) mice. A: At seven days after wounding in C57BL/6HNsd mice, the intramedullary space is filled with reactive woven bone (*). B: At 14 days after wounding, there is woven bone within the wound space and partial repopulation of marrow. Higher power view (inset) shows tartrate-resistant acid phosphatase-positively-stained cells on surfaces of intramedullary bony trabeculae. C: At 21 days after wounding, there is ossification in the cortical wound and repopulation of intramedullary canal with hematopoietic marrow cells. D: At 28 days after wounding, there is bridging of the cortical wound with mature bone. E: At 14 days after wounding in NOD/SCID mice, there is presence in the canal of residual clot and poorly vascularized fibrous tissue, with little evidence of ossification. F: At 28 days after wounding, poorly vascularized fibrous tissue fills the medullary canal. Arrows indicate margins of cortical wound in transverse sections.*

Statistical analysis. Wound diameters are presented as means±SEM and were compared by parametric methods if data were determined to be normally distributed by the Kolmogorov-Smirnov test; otherwise non-parametric methods were used. One-way ANOVA tests were used for multiple groups. Fishers exact test was used to compare groups for fibrosis observations. *p*-Values ≤0.05 were considered significant.

Results

Spontaneous healing of tibial wounds. Histological evaluation of unicortical tibial wounds in C57BL/6NHsd mice showed consistent exuberant healing within weeks after wounding

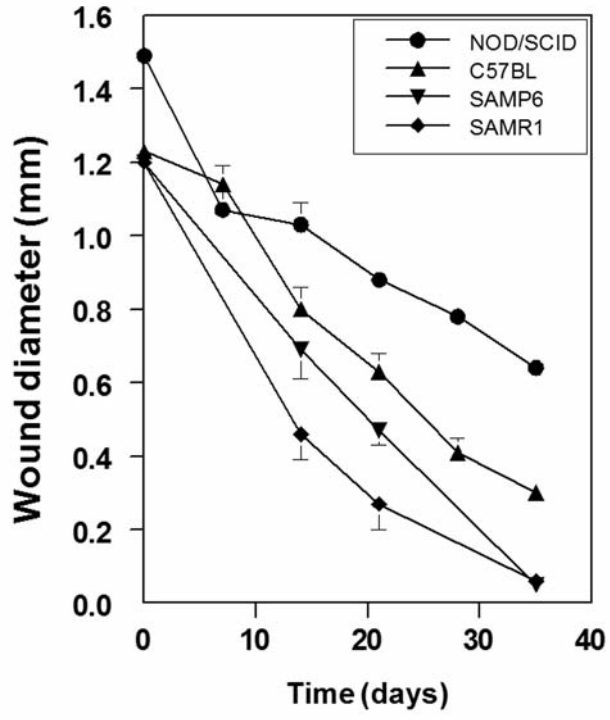

Figure 2. *Radiographic evaluation of healing of unicortical tibial wounds in NOD/SCID mice (n=8-17 at each timepoint), C57BL/6NHsd (n=10-13), SAMP6 (n=12-25), SAMR1 (n=15-29). Wound diameter is presented as the mean±SEM.*

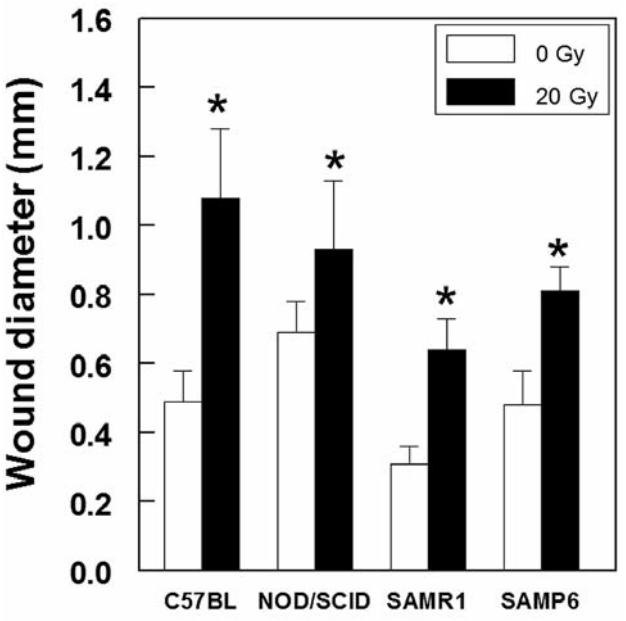

Figure 3. *Comparison of the effects of 20 Gy irradiation to leg one day prior to creation of a unicortical wound in groups of C57BL/6NHsd, NOD/SCID, SAMR1, and SAMP6 mice at 21 days after the creation of wounds. *Statistically significant difference between irradiated and non-irradiated mice for each genotype.*

(Figure 1 A-D). At seven days after wounding, the medullary space was filled with reactive woven bone. At 14 days after wounding, there was evidence of resorption of the reactive intramedullary bone by TRAP-positive cells and re-population of the medullary canal with hematopoietic marrow cells. Enzyme histochemical staining for TRAP activity demonstrated intense activity in multi-nucleated cells on the surfaces of the remaining woven bone. At 21 days after wounding, there was ossification of the cortical wound and complete repopulation of the medullary space with marrow cells. At 28 days after wounding, there was maturation of the architecture of the bone within the cortical wound site.

Genotype-dependent time course of tibial wound healing. Groups of mice showed reproducible rates of wound healing, which were assessed radiographically, but there were marked differences for different genotypes (Figure 2). NOD/SCID mice showed the most gradual rate of osseous wound healing (Figure 1 E-F and Figure 2), such that at 35 days after creation of the wounds, they remained unhealed, with the mean diameter being 0.64±0.09 mm, (43% of the initial diameter). C57BL/6NHsd mice showed progressive wound healing to significantly greater extents than NOD/SCID mice at day 14 (p=0.013), day 21 (p<0.0007), day 28 (p<0.0001), and day 35 (p<0.0001). SAMR1 and SAMP6 mice were tested together and evaluated without identification of the genotype; wounds in SAMR1 mice healed to a greater extent than those in SAMP6 mice at both day 14 and 21 (p<0.05).

Effects of irradiation on tibial wound healing. We assessed the effect of a single dose of irradiation to the right legs of mice 24 h before the creation of tibial wounds. For each genotype there was a statistically significant delay in wound healing (Figure 3). The magnitude of inhibition at day 21 was greatest for C57BL/6NHsd (irradiated wounds 2.2-fold larger than non-irradiated), compared to SAMP6 (2.1-fold), SAMR1 (1.7-fold), and NOD/SCID (1.4-fold). Wounds in irradiated legs showed persistence of clot and fibrosis, with defective in-growth of vessels and neo-osteogenesis (Figure 4A and B). Nevertheless, irradiated wounds showed distinct capacities to recover, with evidence of delayed medullary osteogenesis and bone resorption at day 21 for C57BL/6NHsd mice (Figure 4C and D).

In a time-course study comparing SAMR1 and SAMP6 genotypes (Figure 5A and B), there was a gradual decrease in the size of the wound in both, with both showing delayed wound healing after 20 Gy irradiation to the limb. By day 35, there was evidence of recovery from irradiation for SAMR1 mice. Morphometric analysis at day 21

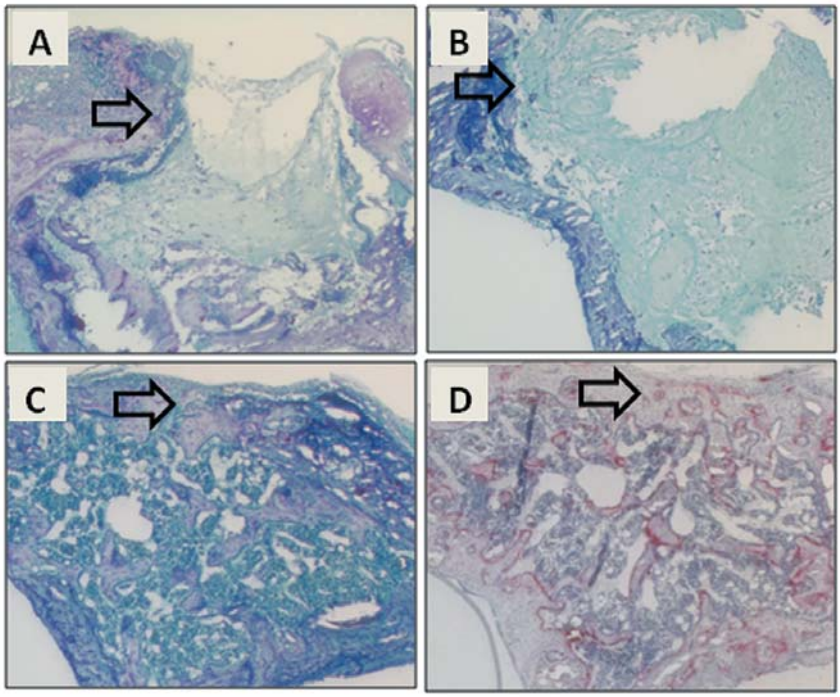

Figure 4. *Delay of wound healing after a single dose of irradiation to legs in C57BL/6NHsd mice. A: Day 7, toluidine blue stain. B: Day 14, toluidine blue stain. C: Day 21, toluidine blue stain. D: Day 21, tartrate-resistant acid phosphatase stain. Arrows indicate a margin of the wound in transverse sections.*

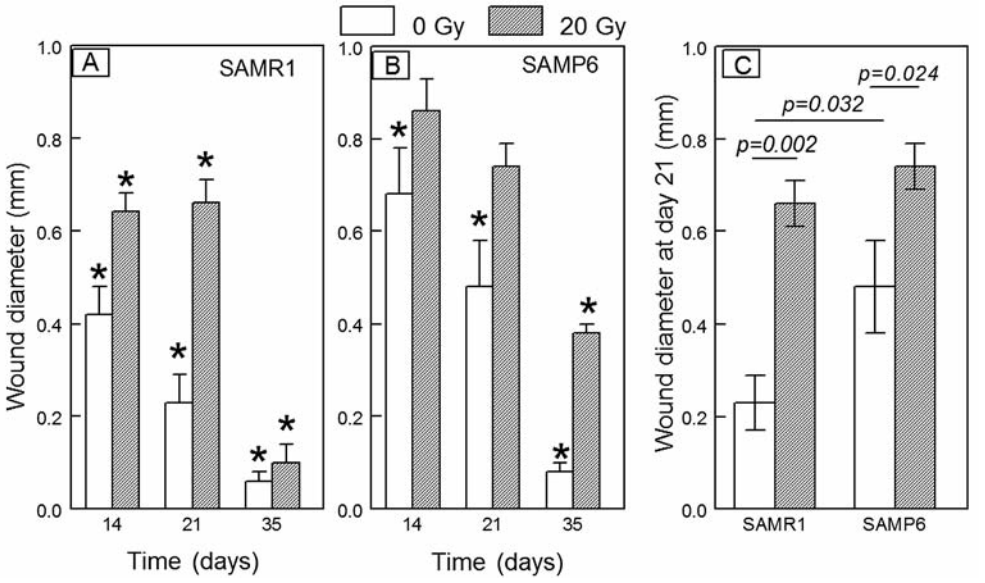

Figure 5. *Comparison of effects of irradiation on osseous wound diameter in SAMR1 and SAMP6 mice at intervals after creation of the wounds. *Statistically significant difference between day 0 and indicated day. Lines indicate the p-values for significant differences between groups.*

(Figure 5C), for example, showed smaller wounds in non-irradiated SAMR1 mice compared to non-irradiated SAMP6 mice (p=0.032). Limb irradiation in SAMR1 mice resulted in larger wounds (p=0.002) than in non-irradiated mice. Likewise, limb irradiation in SAMP6 mice resulted in even larger wounds (p=0.024) than in non-irradiated SAMP6. There was more extensive fibrosis *in lieu* of bone in the irradiated SAMP6 mice (Figure 6E); a greater

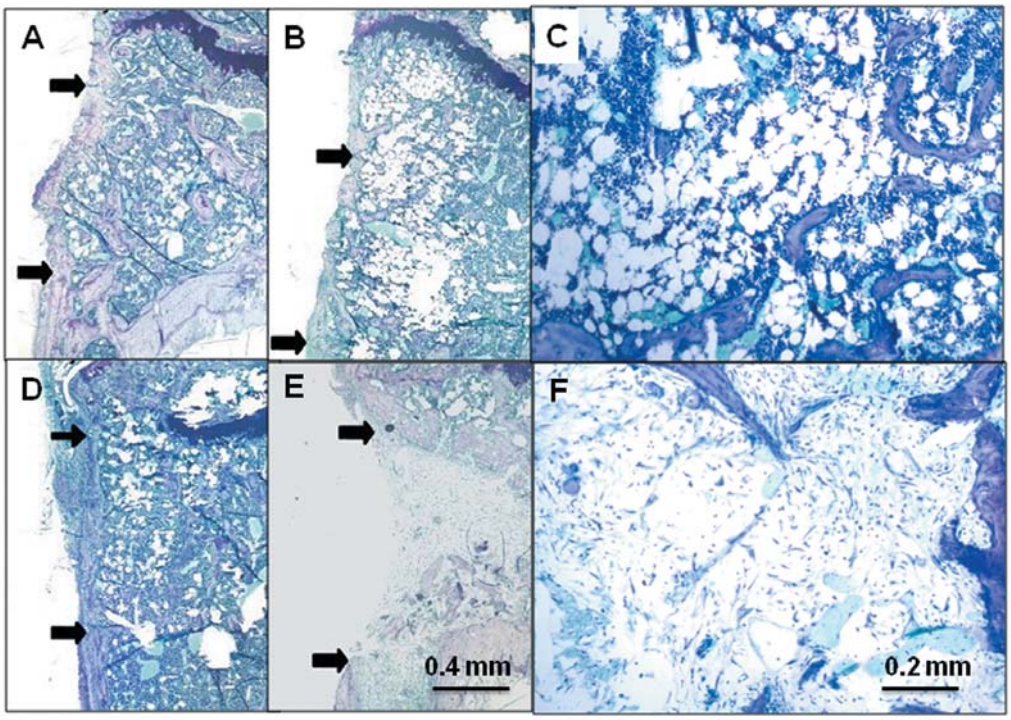

Figure 6. *Comparison of effects of irradiation on osseous wound healing in SAMR1 and SAMP6 mice at 21 days after creation of the wounds. Representative photomicrographs show SAMR1 mice with no irradiation (A) and 20 Gy irradiation (D) to the leg and SAMP6 mice with no irradiation (B, C) and 20 Gy irradiation (E, F) to the leg. Arrows indicate margins of the wound in longitudinal sections.*

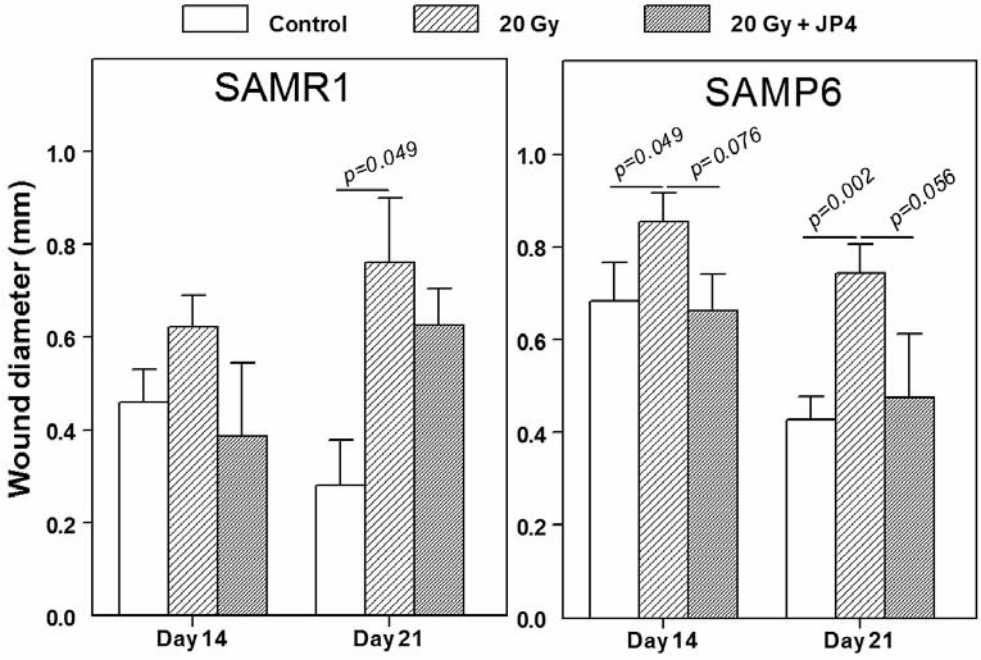

Figure 7. *Effects of irradiation (20 Gy) to the leg with and without a single intraperitoneal dose of JP4-039 on osseous wound healing in SAMR1 and SAMP6 mice. Irradiation and drug administration were carried out 24 h prior to creation of the unicortical tibial wounds.*

number of SAMP6 mice (75%) showed intramedullary fibrosis upon irradiation than did SAMR1 mice (13%, p=0.0013, Table I).

A small experiment was conducted to assess the effect of a single intraperitoneal dose of the GS-nitroxide, JP4-039, on osseous wound healing in irradiated legs (Figure 7). With the numbers of mice available, 6 to 10 per group, there was a borderline significant improvement of wound healing in irradiated limbs in SAMP6 mice, both at 14 days (p=0.076) and 21 days (p=0.056) after creation of the wounds. With smaller numbers of SAMR1 mice, 4-5 per group, the improvement of healing in irradiated tibiae by JP4-039 was not statistically significant (Figure 7). Analysis of wounds in non-irradiated tibiae at day 14 showed 56% smaller wounds (0.25±0.09 mm, n=6) in SAMP6 mice treated with JP4-039 than in untreated SAMP6 mice (0.45±0.03, n=10, p=0.0509). No effect of JP4-039 on wound healing in non-irradiated legs was detected at day 21.

Table I. *Effect of irradiation on incidence of fibrosis in osseous wounds in SAMR1 and SAMP6 mice.*

	0 Gy	20 Gy	p-Value[a]
SAMR1	0% (0/17)	13% (1/8)	0.347
SAMP6	0% (0/32)	75% (12/16)	0.0013

[a]Fisher's test for 0 *vs.* 20 Gy.

Discussion

Spontaneous repair of osseous wounds in this mouse model recapitulates the process of fracture healing as we have previously described for a rat tibial wound model (6). It is characterized by in-growth of vessels and neo-osteogenesis within the medullary canal, osteoclastic resorption of the temporary intramedullary woven bone, restoration of medullary hematopoiesis, and maturation and bridging of the cortical wound. This model of spontaneous bone healing entails a wound location that could be monitored by morphometric analysis of digitized radiographic images. Thus, timepoints could be selected for readily-evaluating treatments that could either accelerate or delay healing. The model was previously used in rats to assess the effects of various bone-substitute materials on bone repair (7). The model was adapted for C57BL/6NHsd mice to assess the effects of different classes of radioprotectors to mitigate irradiation-induced delay in bone wound healing (8).

There were striking differences in the rates of wound healing in various mice genotypes tested here, with SAMR1 mice showing the most rapid healing. The senescence-accelerated mouse (SAM Prone) strains arose spontaneously from the AKR/J background and display shortened life-span and an array of signs of accelerated aging compared to the control SAMR strains (9). In particular, the SAMP6 variant displays approximately 4 months of normal skeletal development and growth, followed by an age-related accelerated decrease in bone mass (10, 15) with increased marrow adiposity (16). Our recent *in vitro* studies on their bone marrow cells were consistent with the oxidative stress mechanism of aging and indicated that impaired proliferation of osteoblast progenitors in SAMP6 marrow may be the major factor contributing to low bone mass (17).

This is a study of bone's capacity for wound healing, in distinction from defect models that test an agent's ability to promote bone formation in an otherwise non-healing lesion. As such, it can identify conditions or agents that interfere with spontaneous bone formation (6, 7). Similar models have been used to assess the effects of irradiation on bone repair in beagles (18) and in rats (19, 20). Such osseous wounds are intended to inflict minimal damage to surrounding tissues and mimic controlled, reproducible surgical procedures. There has been limited investigation of bone healing capacity in SAMP6 mice. There were no discernable differences in bone formation by μ-Computed Tomography or histology between SAMP6 and SAMR1 mice in a study that used a femoral osteotomy model with rigid fixation, although bone marrow cells from the former showed the expected *in vitro* reduction in osteoblast differentiation and increase in adipocyte differentiation (21). That specific model employed a small 0.22-mm gap with internal rigid fixation and relied on periosteal osteogenesis rather than a marrow contribution to callus and healing. Another study with a femur fracture model with less rigid fixation, allowing for endochondral and intra-membranous healing, compared young and old mice (22). Biomechanical and histological analyses revealed a repair delay in 10-month-old and not in 5-month-old SAMP6 mice compared to SAMR1 mice. Thus, differences in bone healing may or may not be detected depending on the age and relative dependence of the model on periosteal osteogenesis. The cortical wound model used here is a model for spontaneous bone formation following osseous injury and is intended to isolate the process of bone formation independent of inflammatory processes, mobility, and damage to soft tissues that are encountered in fractures. This study revealed differences in medullary osteogenesis attributable to marrow progenitors of osteoblasts. It is notable that development of osteopenia in SAMP6 mice can be prevented by transplantation of bone marrow from normal allogeneic mice (23); this suggests that the skeletal defect may be due to dysregulated bone progenitor cells, their products, or other components of marrow. In addition, there is direct evidence from us (17) and others (24, 25) that *in vitro* osteoblast potential is reduced in SAMP6 marrow even if periosteal bone formation is normal (21, 22).

We previously described studies with C57BL/6NHsd mice in which the novel antioxidant gramicidin S-nitroxide, JP4-039, not only ameliorated the irradiation-induced delay in bone wound healing, but also facilitated more rapid bone wound healing in non-irradiated tibias (8). The data described herein in SAMP6 mice, are consistent with those findings and provide evidence that small-molecule antioxidants may be of value in the management of bone fracture healing in osteoporosis. JP4-039 is a unique small molecule formed by coupling hemigramicidin S-segment to the drug tempol (4-hydroxy-2,2,6,6-tetramethylpiperidine-N-oxyl) to target it to the mitochondria for increased scavenging of reactive oxygen species (26). It has been shown to suppress superoxide generation and apoptosis *in vitro*, lethal hemorrhagic shock in rats (27) and effects of lethal irradiation in mice (28, 29).

There is little information regarding the role of antioxidants in bone repair, but some proof-of-principle information has been obtained with standard antioxidants. For example, daily injections of vitamin C mitigated the damaging effect of five days of intraperitoneal injections of zymosan on fracture healing in rats (30) and more rapid bone healing was documented in dogs administered vitamin E daily for one week following radial diaphysis fracture (31). Vitamin E has been considered as "possibly unsafe" at daily intakes of ≥400 IU, being associated with hemorrhagic stroke, cancer, and vision and bleeding disorders (31). Large doses of many antioxidants have been reported as being ineffective at preventing oxidative damage in animal disease models, perhaps because antioxidants cannot penetrate cell membranes effectively and therefore do not reach the relevant sites of reactive oxygen species generation (26).

In summary, these studies show genotype-specific differences in the rate of spontaneous healing of bone wounds and in the sensitivity to a single dose of irradiation. Different mouse genotypes show differences in extents of fibrosis and vascularization in irradiated wounds and may be useful or not depending on the research question. These mouse models should be valuable for determining mechanisms of the effects of irradiation on bone healing and also for the design and testing of novel bone growth-enhancing drugs and mitigators of ionizing irradiation.

Conflicts of Interest

The Authors report no conflicts of interest.

Acknowledgements

This research was funded by NIAID/NIH grant U19A1068021 and NIH R21AG034254.

References

1 Widmann RF, Pelker RR, Friedlaender GE, Panjabi MM and Peschel RE: Effects of prefracture irradiation on the biomechanical parameters of fracture healing. J Orthop Res *11*: 422-428, 1993.

2 Giannoudis PV, Jones E and Einhorn TA: Fracture healing and bone repair. Injury *42*: 549-550, 2011.

3 Nicholls F, Janic K, Filomeno P, Willett T, Grynpas M and Ferguson P: Effects of radiation and surgery on healing of femoral fractures in a rat model. J Orthop Res *31*: 1323-1331, 2013.

4 Aksnes LH and Bruland OS: Some musculo-skeletal sequelae in cancer survivors. Acta Oncol *46*: 490-496, 2007.

5 Jereczek-Fossa BA and Orecchia R: Radiotherapy-induced mandibular bone complications. Cancer Treat Rev *28*: 65-74, 2002.

6 Eid K, Zelicof S, Perona BP, Sledge CB and Glowacki J: Tissue reactions to particles of bone-substitute materials in intraosseous and heterotopic sites in rats: Discrimination of osteoinduction, osteocompatibility, and inflammation. J Orthop Res *19*: 962-969, 2001.

7 Eid K, Chen E, Griffith L and Glowacki J: Effect of RGD-coating on osteocompatibility of PLGA-polymer disks in a rat tibial wound. J Biomed Mat Res *57*: 224-231, 2001.

8 Gokhale A, Rwigema J-C, Epperly MW, Glowacki J, Wang H, Wipf P, Goff JP, Dixon T, Patrene K and Greenberger JS: Small molecule GS-nitroxide ameliorates ionizing irradiation-induced delay in bone wound healing in a novel murine model. In Vivo *24*: 377-385, 2010.

9 Takeda T, Hosokawa M and Higuchi K: Senescence-accelerated mouse (SAM): a novel murine model of senescence. Exp Gerontology *32*: 105-109, 1997.

10 Matsushita M, Tsuboyama T, Kasai R, Okumura H, Yamamuro T, Higuchi K, Higuchi K, Kohno A, Yonezu T and Utani A: Age-related changes in bone mass in the senescence accelerated mouse (SAM). SAM-R/3 and SAM-P/6 as new murine models for senile osteoporosis. Am J Pathol *125*: 276-283, 1986.

11 Ito M, Hiramatsu H, Kobayashi K, Suzue K, Kawahata M, Hioki K, Ueyama Y, Koyanagi Y, Sugamura K, Tsuji K, Heike T and Nakahata T: NOD/SCID/gamma(c)(null) mouse: An excellent recipient mouse model for engraftment of human cells. Blood *100*: 3175-3182, 2002.

12 Rwigema JC, Beck B, Wang W, Doemling A, Epperly MW, Shields D, Goff JP, Franicola D, Dixon T, Frantz MC, Wipf P, Tyurina Y, Kagan VE, Wang H and Greenberger JS: Two strategies for the development of mitochondrion-targeted small molecule radiation damage mitigators. Int J Radiat Oncol Biol Phys *80*: 860-868, 2011.

13 Frantz MC, Pierce JG, Pierce JM, Kangying L, Qingwei W, Johnson M and Wipf P: Large-scale asymmetric synthesis of the bioprotective agent JP4-039 and analogs. Org Lett *13*: 2318-2321, 2011.

14 Fallon MD and Teitelbaum SL: A simple procedure for the rapid histological diagnosis of metabolic bone disease. Calcif Tissue Int *33*: 281-283, 1981.

15 Kasai S, Shimizu M, Matsumura T, Okudaira S, Matsushita M, Tsuboyama T, Nakamura T and Hosokawa M: Consistency of low bone density across bone sites in SAMP6 laboratory mice. J Bone Mineral Metab *22*: 207-214, 2004.

16 Kajkenova O, Lecka-Czernik B, Gubrij I, Hauser SP, Takahashi K, Parfitt AM, Jilka RL, Manolagas SC and Lipschitz DA: Increased adipogenesis and myelopoiesis in the bone marrow of SAMP6, a murine model of defective osteoblastogenesis and low turnover osteopenia. J Bone Miner Res *12*: 1772-1779, 1997.

17 O'Sullivan RP, Greenberger JS, Goff J, Cao S, Kingston KA, Zhou S, Dixon T, Houghton FD, Epperly MW, Wang H and Glowacki J: Dysregulated *in vitro* hematopoiesis, radiosensitivity, proliferation, and osteoblastogenesis with marrow from SAMP6 mice. Exp Hematol *40*: 499-509, 2012.

18 Schlegel d, Hilfrich J, Klemm H and Schreckenberger H: Knochenbregeneration im Tieversuch nach Strahlenbelastung. Electromedica *1*: 26-28, 1972.

19 Melcher AH and Irving JT: The healing mechanisms in artificially created circumscribed defects in the femora of albino rats. J Bone Joint Surg *44B*: 928-936, 1962.

20 Arnold M, Kummermehr J and Trott KR: Radiation-induced impairment of osseous healing: quantitative studies using a standard drilling defect in rat femur. Radiat Res *143*: 77-84, 1995.

21 Egermann M, Heil P, Tami A, Ito K, Janicki P, Von Rechenberg B, Hofstetter W and Richards PJ: Influence of defective bone marrow osteogenesis on fracture repair in an experimental model of senile osteoporosis. J Orthop Res *28*: 798-804, 2010.

22 Histing T, Kuntz S, Stenger D, Scheuer C, Garcia P, Holstein JH, Klein M, Pohlemann T and Menger MD: Delayed fracture healing in aged senescence-accelerated P6 mice. J Invest Surg *26*: 30-35, 2013.

23 Ichioka N, Inaba M, Kushida T, Esumi T, Takahara K, Inaba K, Ogawa R, Iida H and Ikehara S: Prevention of senile osteoporosis in SAMP6 mice by intrabone marrow injection of allogeneic bone marrow cells. Stem Cells *20*: 542-551, 2002.

24 Jilka RL, Weinstein RS, Takahashi K, Parfitt AM and Manolagas SC: Linkage of decreased bone mass with impaired osteoblastogenesis in a murine model of accelerated senescence. J Clin Invest *97*: 1732-1740, 1996.

25 Silva MJ, Brodt MD, Ko M and Abu-Amer Y: Impaired marrow osteogenesis is associated with reduced endocortical bone formation but does not impair periosteal bone formation in long bones of SAMP6 mice. J Bone Miner Res *20*: 419-427, 2005.

26 Wipf P, Xiao J, Jiang J, Belikova NA, Tyurin VA, Fink MP and Kagan VE: Mitochondrial targeting of selective electron scavengers: synthesis and biological analysis of hemigramacidin-TEMPO conjugates. J Am Chem Soc *127*: 12460-12461, 2005.

27 Macias C A, Chiao J W, Xiao J, Arora DS, Tyurina YY, Delude RL, Wipf P, Kagan VE and Fink MP: Treatment with a novel hemigramacidin-TEMPO conjugate prolongs survival in a rat model of lethal hemorrhagic shock. Ann Surg *245*: 305-314, 2007.

28 Jiang J, Kurnikov I, Belikova NA, Xiao J, Zhao Q, Amoscato AA, Braslau R, Studer A, Fink MP, Greenberger JS, Wipf P and Kagan VE: Structural requirements for optimized delivery, inhibition of oxidative stress, and antiapoptotic activity of targeted nitroxides. J Pharmacol Exp Ther *320*: 1050-1060, 2007.

29 Epperly MW, Pierce JG, Dixon T, Franicola D, Wipf P and Greenberger JS: The mitochondrial targeted GS-nitroxide JP4-039 protects against irradiation induced damage *in vitro* and *in vivo*. Exp Hematol *36*: S50-S51, 2008.

30 Duygulu F, Yakan B, Karaoglu S, Kutlubay R, Karahan OI and Ozturk A: The effect of zymosan and the protective effect of various antioxidants on fracture healing in rats. Arch Orthop Trauma Surg *127*: 493-501, 2007.

31 Durmus AS, Akpolat N and Unsaldi E: Effect of DL-α-tocopheral-acetate on the fracture healing of experimental radial diaphysis fracture in dogs. Firat Univ J Health Sciences *22*: 141-146, 2008.

Received December 5, 2013
Revised January 21, 2014
Accepted January 22, 2014